Okajimas Folia Anat. Jpn., **95**(1): 1–7, August, 2018

CBCT imaging of the alveolar bone structure in maxilla of elderly donor cadavers and PCA analysis

By

Rieko ASAUMI[1], Taisuke KAWAI[1], Yoko MIWA[2], Masataka SUNOHARA[2], Iwao SATO[2]

[1]Department of Oral and Maxillofacial Radiology, School of Life Dentistry at Tokyo, The Nippon Dental University, 1-9-20 Fujimi Chiyoda-ku, Tokyo, Japan
[2]Department of Anatomy, School of Life Dentistry at Tokyo, The Nippon Dental University, 1-9-20 Fujimi Chiyoda-ku, Tokyo, Japan

–Received for Publication, January 15, 2018–

Key Words: CBCT, maxilla, alveolar bone, PCA

Summary: There is an important bone matrix with remodelling between dentate and edentulous samples of the human maxilla for bone metabolism. Cone beam computed tomography (CBCT) is useful for structural analysis of bone. The objective of this study was to investigate morphological data of donor cadavers in detail using CBCT imaging and principal component analysis (PCA). We analysed 38 donor cadavers using a CBCT apparatus. The analytical results defined differences in skull measurement parameters and dentate and edentulous levels using PCA. We observed cortical bone, trabecular bone, and the distance from the bottom of the maxillary sinus to the oral mucosa at a right angle to the palatal plane of the first molar region between dentate and edentulous samples of the human maxilla using CBCT imaging. In the dentate sample of the maxilla, component 1 was defined by negative contributions from gender (−0.84) and age (−0.54) to positive contributions such as cortical bone structure (CBS, 0.68) and trabecular bone structure (TBS, 0.50). There was a difference in CBS between dentate and edentulous human maxilla samples. This study of CBCT data provides useful basal information for planning dental implant surgery using PCA.

Introduction

The structure of alveolar bone with cortical bone is important for implant placement in dental treatments in human maxillae and mandibles (Muller et al., 2003; Trombelli et al., 2010; Wirth et al., 2011). In general, cone beam computed tomography (CBCT) imaging is useful for structural analysis of bone matrices and bone metabolism (Väänänen et al., 2011; de Rezende et al., 2016). However, little is known about promoter markers such as CBCT for alveolar bone with cortical and cancellous bone structures in the human maxilla in dentate and edentulous samples. It is clearly an important contributor to alveolar bone structure for a dental implant in dentate and edentulous maxillae. Dental treatment for implants must be carefully performed with respect to the bone structure in dentate and edentulous individuals (Brockhoff et al., 2014; Tozoğlu and Cakur, 2014; Jia and Meng, 2015). However, in previous reports, it has been difficult to identify correlation levels among bone matrices and other elements such as gender and age. Moreover, we need to investigate differences between dentate and edentulous samples in the human maxilla. Principal component analysis (PCA) is a statistical procedure that uses an orthogonal transformation to convert a set of observations of possibly correlated variables into a set of values of linearly uncorrelated variables, called principal components (Cassar-Malek, 2007). Therefore, we attempted to perform CBCT analysis of the bone structure of the human maxillary alveolar bone in human cadavers using PCA.

Material and Methods

Sample preparation

Thirty-eight Japanese cadavers from the Department of Anatomy of the Nippon Dental University were used in this study. These included sixteen male cadavers (65–90

Corresponding author: Iwao Sato, Department of Anatomy, School of Life Dentistry at Tokyo, The Nippon Dental University. 1-9-20 Fujimi Chiyoda-ku, Tokyo, Japan. E-mail: iwaoa1@tokyo.ndu.ac.jp

years old; mean, 80.3 years) and twenty-two female cadavers (66–97 years old; mean, 88.2 years old). Seventy-six sides (dentate samples: 14 males, 12 females; edentulous samples: 18 males, 32 females) of the maxilla were observed. The maxillary first molar region was investigated. Subjects with bone disease, especially osteoporosis (Barngkgei et al., 2014), and partially damaged or already-dissected maxillae were excluded from our study.

CBCT analysis

The CBCT system used for scanning images was the AZ 3000CT (Asahi Roentgen Industry, Kyoto, Japan). The scan structure was as follows: the tube voltage was 85 kV, the tube current was 4 mA, the scanning time was 17 seconds, the field of view (FOV) was 79 mm φ × 80 mm H, and the voxel size was 0.155 × 0.155 × 0.155 mm. NEOPREMIUM software (Asahi Roentgen Industry, Kyoto, Japan) was used to generate CBCT images from CBCT data. The images were observed in the palatal plane as a horizontal reference plane. Ten sides that showed heavy bone resorption and four sides that were removed during radical operations of the maxillary sinus were excluded from the CBCT observation. Then, the frontal position was used for the infra-zygomatic crest in specimens without first molars and the location between the first molar and second molar in specimens with first molars (Fig. 1). Then, the cross-sectional images of the maxillary alveolar bone at each frontal position were reconstructed (Fig. 1). Sixty-one sides (dentate samples: 9 males, 12 females; edentulous samples: 18 males, 22 females) of the maxilla were observed for CBCT analysis, except for large resorption bone matrix samples.

Classification types of bone structure between cortical bone and cancellous bone of the maxilla from CBCT images

Measurements were assessed using ImageJ 1.48 (Ras-

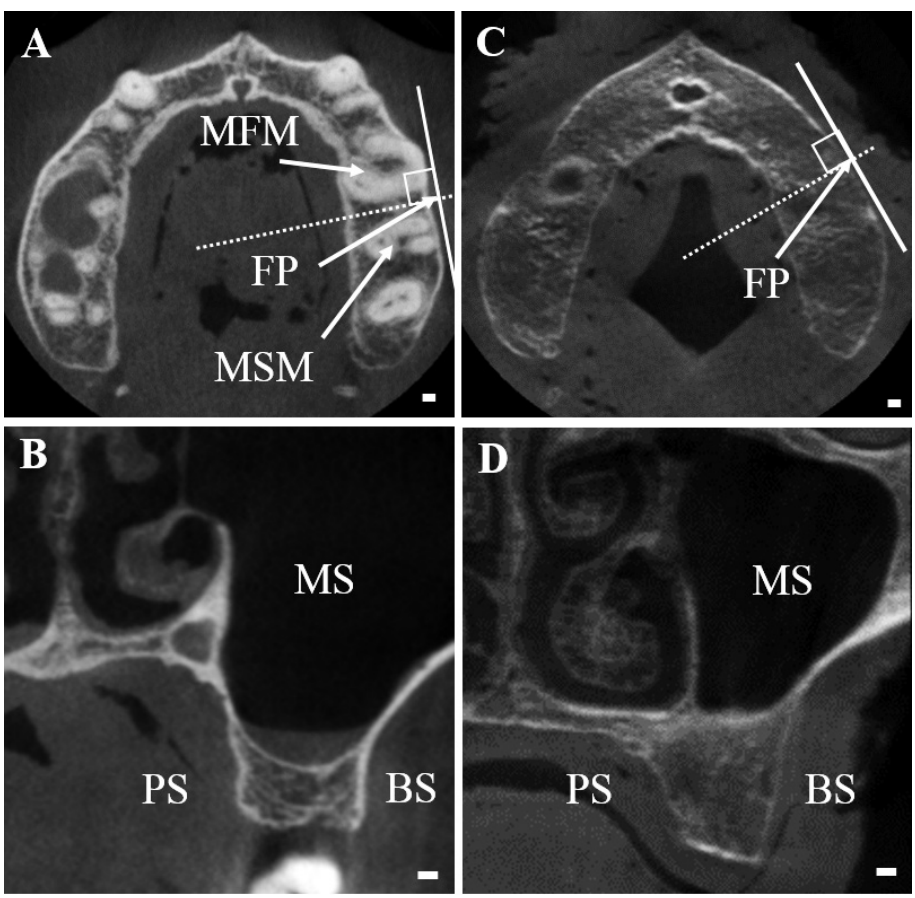

Fig. 1. (A) Axial CBCT image of the dentate human maxilla for positioning of the cross-sectional image. FP is the position between MFM and MSM of the dentate human maxilla. The dotted line is the mesio-distal position for Fig. 1B. The dotted line is also at a right angle to the palatal plane. (B) Cross-sectional CBCT image of the left side of the dentate human maxilla for analysis. (C) Axial CBCT image of the edentulous human maxilla for positioning of the cross-sectional image. FP is the position of the infrazygomatic crest of the edentulous human maxilla. The dotted line is the mesio-distal position for Fig. 1D. The dotted line is also at a right angle to the palatal plane. (D) Cross-sectional CBCT image of the left side of the edentulous human maxilla for analysis. MFM: Maxillary first molar, MSM: Maxillary second molar, FP: Frontal point, MS: Maxillary sinus, PS: Palatal side, BS: Buccal side, Bar = 2 mm

band 1997–2015). Cross-sectional images of the maxillary alveolar bone were observed. The specimens were selected according to the following inclusion criteria for height classification of the alveolar bone (Tozoğlu and Cakur, 2014; Misch, 2015) (Fig. 1): less than 5 mm or 5 mm or more in all examined specimens (Fig. 2). We also defined two classes (Class I and Class II) for the distance from the bottom of the maxillary sinus to the oral mucosa at a right angle to the palatal plane of the first molar region (DBM-O) (Fig. 2) as follows: Class I, distance of 5 mm or more; and Class II, distance of less than 5 mm. We assessed and classified the specimens based on two structures (type 1 and type 2) (Fig. 2) of cortical bone structure (CBS) and four types (A-D) of trabecular bone structure (TBS) (Fig. 2) of cancellous bone as follows: type 1, clear CBS; type 2, unclear CBS with hard calcification bone matrices; type A, parallel-arranged elongated TBS; type B, mesh TBS; type C, loose TBS; and type D, compacted detection of

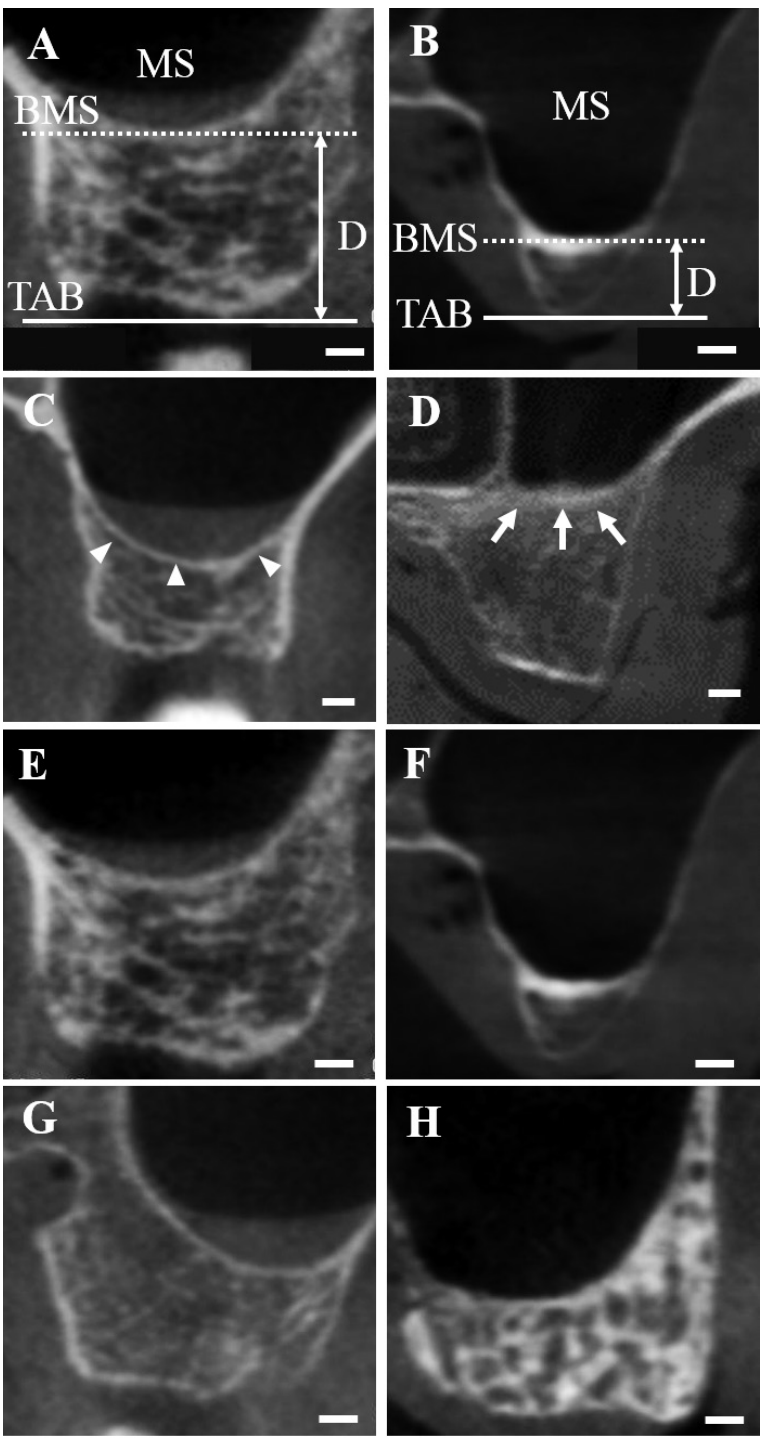

Fig. 2. (A) Cross-sectional CBCT image showing alveolar bone with a height of 5 mm or more (Class I). (B) Cross-sectional CBCT image showing alveolar bone with a height of less than 5 mm (Class II). (C) CBCT image of the Type 1 human maxilla. The alveolar bone indicated a clear cortical bone structure (arrowheads). (D) CBCT image of the Type 2 human maxilla. The alveolar bone indicated an unclear cortical bone structure (arrows). (E) CBCT image of the Type A human maxilla. The alveolar bone was composed of a parallel-arranged elongated TBS. (F) CBCT image of the Type B human maxilla. The alveolar bone was composed of a mesh TBS. (G) CBCT image of the Type C human maxilla. The alveolar bone was composed of a loose TBS. (H) CBCT image of the Type D human maxilla. The alveolar bone was composed of a compacted calcified bone matrix. MS: maxillary sinus, BMS: bottom of the maxillary sinus, TAB: top of the alveolar bone, D: distance between BMS and TAB, Bar = 2 mm.

calcified bone matrix (Fig. 2).

Statistical analysis

The differences in bone structure and density among the forms were assessed using Student's t-test and a two-way analysis of variance (ANOVA), followed by Tukey's post hoc test. Differences were considered significant when $p < 0.05$. The results are reported as the mean ± SD. We performed multivariate modelling by quantitative data principal component analysis (PCA) to estimate the interaction between measured elements of the human maxilla (Cassar-Malek et al., 2007). The groups were assessed using ANOVA followed by Bonferroni's post hoc test with one categorical independent variable and one continuous variable (the independent variable can consist of a number of groups). The statistical analyses were performed using IBM SPSS statistics software (Base, version 22) (New York, USA).

Ethics

The study was approved by the Human Research Committee of Nippon Dental University (no. NDU-T2015-20). The human cadavers were obtained from a donor-based system using the guidelines included in the Law Concerning Body Donation for Medical and Dental Education (the Body Donation Law) and the Law Concerning Cadaver Dissection and Preservation (LCCDP). The authors declare no conflicts of interest related to the study.

Results

Analysis of the maxillary bone structure classification (see Fig. 2)

The classifications of the human maxillary bone structures are shown in Table 1. Maxillary alveolar bone distance of 5 mm or more (Class I, Fig. 2) was found on 48 sides (78.7%, 48/61; dentate, 29.5%, 18/61; edentulous, 49.2%, 30/61), in contrast with the distance of less than 5 mm (Class II), which was found on 13 sides (21.3%, 13/61, dentate, 4.9%, 3/61, edentulous, 16.4%, 10/61). Type 1 (Fig. 2) CBS of the maxillary alveolar bone was seen in 28 sides (45.9%, 28/61; dentate, 16.4%, 10/61, edentulous, 29.5%, 18/61), and Type 2 CBS of the maxillary alveolar bone was seen in 33 sides: 54.1%, 33/61 (dentate, 18.0%, 11/61; edentulous, 36.0%, 22/61). The four types (A-D, Fig. 2) of cancellous bone were defined as follows: dentate samples: type A, 13.1% (8/61); type B, 3.3% (2/61); type C, 4.9% (3/61); and type D, 13.1% (8/61). By contrast, edentulous samples of the maxilla were distributed as follows: type A, 3.3% (2/61); type B, 21.3% (13/61); type C, 13.1% (8/61); and type D, 27.9% (17/61). The following correlation was found among the measurements of the dentate samples: a positive correlation between TBS and CBS ($r = 0.754$, $p < 0.05$) by Pearson's correlation coefficient (Table 2). In contrast, type B (male) and type C (female) of TBS were significantly frequent in the edentulous samples ($p < 0.05$) by Pearson's Chi-square test (Table 3). Moreover, CBS was more frequent in males of the edentulous samples ($p < 0.05$) by Pearson's Chi-square test (Table 4).

PCA analysis

PCA analysis was performed for human maxilla measurements data for the following five elements: age, gender, CBS, TBS, and DBM-O. PCA was used to estimate the internal relationship between these elements in the human maxilla (Fig. 3). The two principal components significantly explained 64.1% (component 1: 38.4%; component 2: 25.7%) of the dentate samples ($n = 21$). Figure 3 shows the projection of the variables on components 1 and 2 of the two-dimensional map between dentate and edentulous samples of the human maxilla (Table 4). In the dentate sample of the maxilla, component 1 was characterized by negative contributions from gender (−0.51) and

Table 1. Morphological features of the human maxilla at the first molar region.

		Dentate		Edentulous	
		Male	Female	Male	Female
DBM-O	Class I	8 (13.1%)	10 (16.4%)	15 (24.6%)	15 (24.6%)
	II	1 (1.6%)	2 (3.3%)	3 (4.9%)	7 (11.5%)
CBS	Type 1	3 (4.9%)	7 (11.5%)	5 (8.2%)	13 (21.3%)
	2	6 (9.8%)	5 (8.2%)	13 (21.3%)	9 (14.8%)
TBS	Type A	2 (3.3%)	6 (9.8%)	1 (1.6%)	1 (1.6%)
	B	1 (1.6%)	1 (1.6%)	8 (13.1%)	5 (8.2%)
	C	1 (1.6%)	2 (3.3%)	0 (0%)	8 (13.1%)
	D	5 (8.2%)	3 (4.9%)	9 (14.8%)	8 (13.1%)

Table 2. Correlation coefficients between measurement properties.

	Dentate				
	Gender	Age	DBM-O	CBS	TBS
Gender	1	0.341	−0.114	−0.099	−0.176
Age	0.341	1	0.238	0.206	0.223
DBM-O	−0.114	0.238	1	−0.221	−0.076
CBS	−0.099	0.206	−0.221	1	0.754**
TBS	−0.176	0.223	−0.076	0.754**	1
	Edentulous				
	Gender	Age	DBM-O	CBS	TBS
Gender	1	0.563**	−0.318*	−0.329*	0.023
Age	0.563**	1	0.119	−0.026	−0.022
DBM-O	−0.318*	0.120	1	0.286	0.023
CBS	−0.329*	−0.026	0.286	1	0.375*
TBS	0.023	−0.022	0.023	0.375*	1

** significant at $p < 0.01$, * significant at $p < 0.05$ by Pearson correlation coefficient.

Table 3. Tabulated statistics: Gender, TBS.

Dentate			TBS				Total
			A Type 1: horizontality	B Type 2: mesh	C Type 3: vague	D Type 4: harden	
Gender	Male	Actual values	2	1	1	5	9
		Expected values	3.4	0.9	1.3	3.4	9
	Female	Actual values	6	1	2	3	12
		Expected values	4.6	1.1	1.7	4.6	12
Total		Actual values	8	2	3	8	21
		Expected values	8	2	3	8	21

λ square test computes $p = 0.484$

Edentulous			TBS				Total
			A Type 1: horizontality	B Type 2: mesh	C Type 3: vague	D Type 4: harden	
Gender	Male	Actual values	1	8	0	9	18
		Expected values	0.9	5.9	3.6	7.7	18
	Female	Actual values	1	5	8	8	22
		Expected values	1.1	7.2	4.4	9.4	22
Total		Actual values	2	13	8	17	40
		Expected values	2	13	8	17	40

λ square test computes $p = 0.038$

positive contributions from CBS (0.90) and TBS (0.91). By contrast, component 2 was characterized by positive contributions from age (0.90) and TBM-O (0.58) (Table 4). In edentulous maxillary samples of component 1, we observed negative contributions of gender (−0.84) and age (−0.54) to positive contributions such as CBS (0.68) and TBS (0.50). By contrast, component 2 was characterized by positive contributions from age (0.70), CBS (0.50), and TBS (0.57) (Table 4). The variables were plotted in a two-dimensional space defined by the two axes of component 1 (x-axis) and component 2 (y-axis) (Fig. 3a, b; Table 5).

Table 4. Tabulated statistics: gender, CBS.

Edentulous			CBS		Total
			Type 1 clearly	Type2 unclearly	
Gender	male	Actual values	5	13	18
		Expected values	8.1	9.9	18
	female	Actual values	13	9	22
		Expected values	9.9	12.1	22
Total		Actual values	18	22	40
		Expected values	2	22	40

λ square test computes $p = 0.048$

Dentulous			CBS		Total
			Type 1 clearly	Type2 unclearly	
Gender	male	Actual values	3	6	9
		Expected values	4.3	4.7	9
	female	Actual values	7	5	12
		Expected values	5.7	6.3	12
Total		Actual values	10	11	21
		Expected values	10	11	21

λ square test computes $p = 0.256$

Discussion

Bone density and quality provided useful information for bone strength, volume, density and quality (Mallya and Tetradis, 2014). The TBS and density of the maxillary alveolar bone must be maintained by bone metabolism. By contrast, there was no correlation between TBS and primary stability (Rozé et al., 2009). Therefore, it is necessary to balance bone structure levels between cortical bone and cancellous bone because the different structures are disturbed by a defective connective tissue volume of mucosa located in the maxilla. The maxilla contains the maxillary sinus with a sinus membrane such as Schneider's membrane. We found a significant feature of CBSs with cancellous bone structure patterns in the dentate

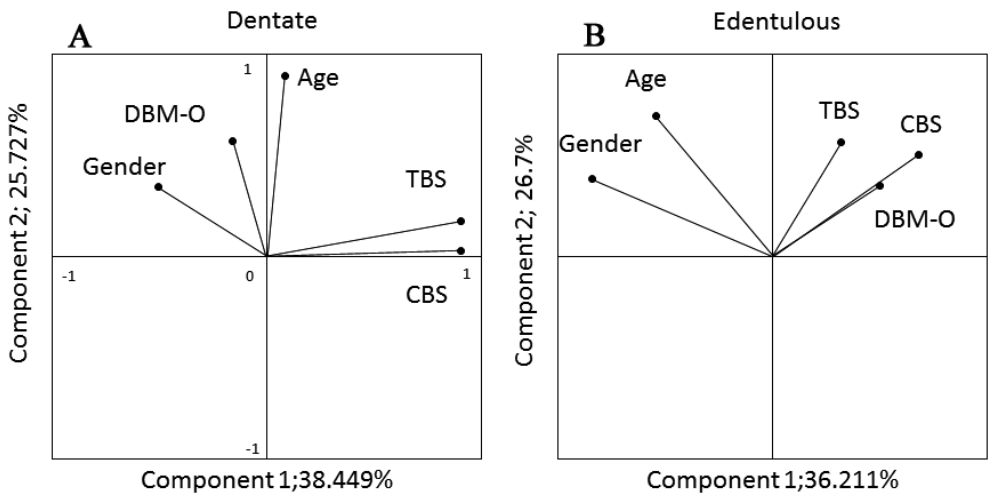

Fig. 3. Variable factor map obtained in all individual samples of the human maxilla by PCA. The original variables are the projected dimension space defined by component 1 (x-axis) and component 2 (y-axis) in dentate and edentulous human maxilla samples. A: dentate sample, B: edentulous sample; DBM-O: the palatal plane of the first molar region, CBS: cortical bone, TBS: trabecular bone structure.

Table 5. Correlations of the original variables with the two main components derived from the principal component analysis in edentulous and dentulous alveolar bone.

	Dentate	
	Component 1	Component 2
Gender	−0.505	0.346
Age	0.084	0.896
DBM-O	−0.158	0.575
CBS	0.902	0.031
TBS	0.906	0.179

The variance of components 1 and 2 are 38.45% and 25.73%, respectively.

	Edentulous	
	Component 1	Component 2
Gender	−0.839	0.386
Age	−0.540	0.698
DBM-O	0.498	0.352
CBS	0.682	0.503
TBS	0.320	0.567

The variance of components 1 and 2 are 36.21% and 26.70%, respectively.

and edentulous samples. In our results, the TBS formed a mesh or parallel-arranged elongated TBS in cancellous bone of the alveolar bone in the dentate sample compared with that of the edentulous sample, with a hard, calcified structure or thin TBS with no formed trabecular bone networks. Therefore, compacted TBS is an important quality of bone structure, which has been supported by previous reports (Muller, 2003; Wirth et al., 2011; de Oliveira, 2012). Our results showed the development of a network of TBS such as types A-D. The fat tissue of cancellous bone is important for bone quality, as shown in previous reports (Beresford et al., 1992; Wang et al., 2016). Statistical analysis using PCA indicated that the contributions of CBS and TBS were the most important markers of bone structure in edentulous samples, in contrast with those of the dentate samples in the male human maxilla and compared with those of the female samples in our study. Therefore, these bone structures must be examined in detail for clinical treatment with dental implants. Moreover, cortical alveolar bone undergoes mechanical stress during mastication. Flanagan (2008) reported that the thickness of cortical bone differed between the buccal and lingual portions of the alveolar bone in the human maxilla. This difference was due to bone metabolism between the TBSs and the density of the alveolar bone.

Conclusion

We analysed the bone structure and density of cortical and cancellous bone between the dentulous and edentulous first molar regions of the maxilla. PCA analysis suggested a correlation between TBS and CBS of the human male maxilla.

Conflict of interest statement

The authors declare that they have no conflict of interest.

References

1) Muller R: Bone microarchitecture assessment: current and future trends. Osteoporos Int 2003; **14**(Suppl 5)**:**89–99.
2) Trombelli L, Minenna P, Franceschetti G, Minenna L, Farina R: Transcrestal sinus floor elevation with a minimally invasive technique. J Periodontol 2010; **81:**158–166.
3) Wirth AJ, Goldhahn J, Flaig C, Arbenz P, Muller R, van Lenthe GH: Implant stability is affected by local bone microstructural quality. Bone 2011; **49:**473–478.
4) Väänänen SP, Isaksson H, Julkunen P, Sirola J, Kröger H, Jurvelin JS: Assessment of the 3-D shape and mechanics of the proximal femur using a shape template and a bone mineral density image. Biomech Model Mechanobiol 2011; **10:**529–538.
5) de Rezende Barbosa GL, Wood JS, Pimenta LA, Maria de Almeida S, Tyndall DA: Comparison of different methods to assess alveolar cleft defects in cone beam CT images. Dentomaxillofac Radiol 2016; **45:**20150332.
6) Brockhoff HC 2nd, Yates DM, Finn R, Phillips C: Comparison of intraoral harvest sites in the edentulous versus dentate specimen. Oral Surg Oral Med Oral Pathol Oral Radiol 2014; **117:**575–580.
7) Tozoğlu U, Cakur B: Evaluation of the morphological changes in the mandible for dentate and totally edentate elderly population using cone-beam computed tomography. Surg Radiol Anat 2014; **36:**643–649.
8) Jia X, Hu W, Meng H: Relationship of central incisor implant placement to the ridge configuration anterior to the nasopalatine canal in dentate and partially edentulous individuals: a comparative study. Peer J 2015; e1315.
9) Cassar-Malek I, Picard B, Kahl S, Hocquette JF: Relationships between thyroid status, tissue oxidative metabolism, and muscle differentiation in bovine fetuses. Domest Anim Endocrinol 2007; **33:**91–106.
10) Barngkgei I, Al Haffar I, Khattab R: Osteoporosis prediction from the mandible using cone-beam computed tomography. Imaging Sci Dent 2014; **44:**263–271.
11) Misch CE: Bone density: A key Determinant for Treatment Planning. In: Misch CE ed, Dental implant prosthetics, 2nd edn. Elsevier Health Sciences, St. Louis, 2015; 237–252.
12) Mallya MS, Tetradis S: Cone-beam computed tomography: Anatomy, In: White SC: Pharoah MJ eds, Oral radiology: principles and interpretation, 7th edn. Elsevier Health Sciences, St. Louis, 2014; 214–228.
13) Rozé J, Babu S, Saffarzadeh A, Gayet-Delacroix M, Hoornaert A, Layrolle P: Correlating implant stability to bone structure. Clin Oral Implants Res 2009; **20:**1140–1145.
14) de Oliveira RC, Leles CR, Lindh C, Ribeiro-Rotta RF: Bone tissue microarchitectural characteristics at dental implant sites. Part 1: identification of clinical-related parameters. Clin Oral Implants Res 2012; **23:**981–986.
15) Beresford JN, Bennett JH, Devlin C, Leboy PS, Owen ME: Evidence for an inverse relationship between the differentiation of adipocytic and osteogenic cells in rat marrow stromal cell cultures. J Cell Sci 1992; **102:**341–351.
16) Wang C, Meng H, Wang X, Zhao C, Peng J, Wang Y: Differentiation of bone marrow mesenchymal stem cells in osteoblasts and adipocytes and its role in treatment of osteoporosis. Med Sci Monit 2016; **22:**226–233.
17) Flanagan D: A comparison of facial and lingual cortical thicknesses in edentulous maxillary and mandibular sites measured on computerized tomograms. J Oral Implantol 2008; **34:**256–258.

Abbreviations

CBS: cortical bone structure
CBCT: cone beam computed tomography
DBM-O: oral mucosa at a right angle to the palatal plane of the first molar region
PCA: principal component analysis
TBS: trabecular bone structure